Tumor Biol. (2016) 37:4203–4212
DOI 10.1007/s13277-015-4029-3

RESEARCH ARTICLE

Curcumin induces apoptosis in p53-null Hep3B cells through a TAp73/DNp73-dependent pathway

Jinhong Wang · Hai Xie · Feng Gao · Tingkun Zhao · Hongming Yang · Bai Kang

Received: 9 October 2014 / Accepted: 27 November 2014 / Published online: 22 October 2015

Abstract Curcumin has anticancer functions in various tumors. It has been shown to induce apoptosis through p53-dependent pathways. p73 gene is a member of the p53 family which encodes both a tumor suppressor (transactivation-competent p73 (TAp73)) and a putative oncogene (dominant-negative p73 (DNp73)); the former shares similarity with the tumor suppressor p53, and the latter behaves as dominant-negative proteins that interfere with the activity of TAp73. To understand the p73-dependent mechanisms that are engaged during curcumin-induced apoptosis, we established a p73 overexpression cell models using p53-deficient Hep3B cells ($Hep3B^{TAp73/DNp73}$). Our results demonstrated that curcumin at concentrations of 40 and 80 μM induced DNA damage, increased TAp73/DNp73 ratio, and also led to apoptosis in the $Hep3B^{TAp73/DNp73}$ cells. The apoptotic cell death was concurrent with the loss of mitochondrial membrane potential; release of cytochrome c from mitochondria; and the cleavage of caspase 9, caspase 3, and poly(ADP-ribose) polymerase (PARP). These results demonstrated a p73-dependent mechanism for curcumin-induced apoptosis that involves the mitochondria-mediated pathway.

Keywords Curcumin · TAp73 · DNp73 · DNA damage · Apoptosis

J. Wang (✉) · F. Gao · T. Zhao · H. Yang · B. Kang
Department of Pharmacology, Weifang Medical University, Weifang 261053, China
e-mail: jinrongwangwf@126.com

H. Xie
Department of Nuclear Medicine, Weifang Medical University, Weifang 261053, China

Abbreviations

BAX	BCL-2-associated X protein
BCL-2	B-cell leukemia/lymphoma 2
MMP	Mitochondrial membrane potential
TAp73	Transactivation-competent p73
DNp73	Dominant-negative p73

Introduction

Curcumin is a diferuloylmethane derived from the dried ground rhizome of the perennial herb curcuma species *Curcuma longa*. Curcumin has been used for centuries in traditional Indian and Chinese medicine. Recent studies show that curcumin possesses potent anti-inflammatory, anti-oxidant, chemo-preventive, and chemo-therapeutic activities [1, 2]. In vitro treatment, curcumin suppresses the proliferation of a variety of cancer cells, including carcinomas of the breast, prostate, esophagus, pancreas, kidney, brain, and lung [3–7].

The tumor suppressor p53 is a transcription factor that is activated by cellular stresses such as DNA damage and oncogene stimulation [8]. Upon activation, p53 may induce cell cycle arrest, DNA repair, cellular senescence, and apoptosis [9, 10]. Thus, p53 acts to maintain genome stability and eliminate damaged or abnormally proliferating cells. Following cellular stresses, p53 is stabilized and binds to DNA as a tetramer, in a sequence-specific manner that results in the transcriptional activation of a series of target proteins including p21, BCL-2-associated X protein (BAX), BCL-2 antagonist killer, and B-cell leukemia/lymphoma 2 (BCL-2) [11–14]. Previous studies have also demonstrated important roles for p53 in curcumin-induced apoptosis. For instance, curcumin can induce human HT-29 colon adenocarcinoma cell apoptosis by activating p53 and regulating apoptosis-related protein

expression [15, 16]. In another case, curcumin treatment can improve the general health of patients with colorectal cancer via the mechanism of increased p53 molecule expression in tumor cells and consequently speeds up tumor cell apoptosis [17]. Unfortunately, loss of p53 function is the most common event during tumorigenesis in diverse types of human cancer; thus, many tumor cells lack the functional p53 [18, 19]. However, little is known about the function of curcumin in p53-mutant (or deficient) cancer cells.

p73, as a p53 family member, is also responsive to the DNA damage that leads to apoptosis [20, 21]. The p73 gene encodes two isoforms that differ in their N-termini and which can be functionally classified as transactivation-competent (TAp73) and dominant-negative (DNp73) proteins [22, 23]. The TAp73 shares similarities with p53 with regard to DNA damage-induced apoptosis through its activation of p53-responsive genes [24, 25]. The DNp73 has a very important regulatory role, as it exerts a dominant-negative effect on p53 and TAp73 by inhibiting their transactivation activity. Thus, DNp73 confers drug resistance to tumor cells harboring p53 and/or TAp73 [24]. Its inhibitory function is exerted either at the oligomerization level, or by competing for binding to the p53/TAp73 DNA target sequence [26]. In addition, the DNp73 promoter contains an efficient p53/TAp73-responsive element that can be transactivated by p53 and/or TAp73, and therefore creates a dominant-negative feedback loop that regulates the function of p53 and/or TAp73 [27, 28]. Several lines of evidences indicate that the presence and participation of different spliced forms of p73 might be one reason for the different cell fates observed in response to DNA damage [29, 30]. However, it is still unknown whether TAp73 and/or DNp73 participates in curcumin-induced apoptosis.

Release of cytochrome c from mitochondria is a key initiative step in mitochondria-dependent apoptosis, and the release of cytochrome c from mitochondria into the cytosol is fundamental to apoptosome formation and initiator caspases (such as caspase 9) and executioner caspases (such as caspase 3) activation [31]. The activated caspase 9 and caspase 3 in turn cleave a variety of cellular substrates, most notably poly(ADP-ribose) polymerase (PARP) [32]. One of the most important functions of PARP is to help repair single-strand DNA nicks. Thus, cleaved PARP is a useful marker of mitochondria-dependent apoptosis [33].

In this current study, we sought to analyze the p73 roles during curcumin-induced apoptosis. Using the p53-deficient and little p73 expression Hep3B cells, we first established a curcumin-induced apoptotic model. Then, we carried out a set of analyses assessing cell viability, percentages of apoptotic cells, extent of DNA damage, and mitochondrial membrane potentials (MMP). Finally, we analyzed the protein levels of TAp73, DNp73, pro-caspase 9, cleaved caspase 9, pro-caspase 3, cleaved caspase 3, pro-PARP, cleaved PARP, and cytochrome c. Our results, as detailed below, suggest that there exists a p53-independent but p73-dependent apoptotic pathway in response to curcumin exposure, which is mediated through the mitochondrial pathway.

Materials and methods

Reagents

Dulbecco's modified Eagle's medium (DMEM) and fetal bovine serum (FBS) were purchased from Gibco Invitrogen Corp. (Gibco Laboratories, Grand Island, NY, USA). 3-(4,5-dimethylthiazol-2-yl)-2,5-diphenyl-2H-tetrazolium bromide (MTT), curcumin, and propidium iodide (PI) were purchased from Sigma-Aldrich (USA). The nucleus/nucleus-free cytosol protein isolation kit was supplied by KeyGEN (Nanjing, China). Expression plasmids for human TAp73 and DNp73 have been described previously [34]. Primer sequences were 5-TGCTGTACGTCGGTGACC-3 (sense DNp73), 5-CGAC GGCTGCAGAGCGAG-3 (sense TAp73), and 5-TCG AAG GTG GAGCTGGGTTG-3 (antisense for both). TAp73, DNp73, and β-actin antibodies were obtained from Santa Cruz Biotechnology (Santa Cruz, CA, USA). Messenger RNA (mRNA) extracted kit and SYBR Green I mix (for quantitative PCR (Q-PCR)) were supplied by Qiagen and Invitrogen, respectively. Caspase 9 and caspase 3 antibodies, as well as IRDye-conjugated anti-rabbit and anti-mouse secondary antibodies, were purchased from Bioworld Technology (St. Louis Park, MN, USA). Cytochrome c antibody and the mitochondria-free cytosol protein isolation kit were supplied by Boster (Wuhan, China), and the annexin V-fluorescein isothiocyanate (FITC)/propidium iodide (PI) apoptosis detection kit was obtained from MultiSciences Biotechnology (Hangzhou, China).

Cell culture and treatment

Hep3B cells were supplied by the Cell Bank of Type Culture Collection of the Chinese Academy of Science (Shanghai, China). Hep3B cells were cultured in DMEM medium which contained 10 % (*v*/*v*) FBS. The cells were cultured at 37 °C in a humidified 5 % CO_2 atmosphere. Curcumin was dissolved in dimethyl sulfoxide (DMSO) to make a stock solution (final concentration: 80 mM).

Establishment of TAp73- and DNp73-overexpressing Hep3B cells ($Hep3B^{TAp73/DNp73}$)

For transfection of the plasmid, Hep3B cells were seeded at 3×10^5 per well in six-well plates. Then, the adherent cells were trypsinized by 0.25 % trypsin and diluted in the DMEM. Lipofectamine 2000 transfection reagent was diluted into Opti-MEM I medium (final concentration: 5 %) and incubated

at room temperature for 10 min. The plasmids were also diluted into Opti-MEM I medium (final concentration 50 nM). Diluted Lipofectamine 2000 transfection agent and diluted plasmid were combined and incubated at room temperature for an additional 20 min. The transfection mixture was added to six-well plates. Cell suspensions were overlaid onto the transfection complexes. After 6-h incubation, the medium was removed and the cells were cultured in normal medium. Q-PCR and Western blotting were performed to validate the transfected efficiency.

Assessment of cell viability

Cell viability was determined by the mitochondrial-dependent reduction of MTT as previously described [35]. Both Hep3B and Hep3B$^{TAp73/DNp73}$ cells were seeded in 96-well plates at 5×10^3 cells per well. Twenty-four hours after plating, cells were treated with curcumin at concentrations of 10, 20, 40, and 80 μM. At 24 h after treatment, the supernatant was removed and 100 μl (500 μg/ml) MTT solution was added to each well. After 4 h of incubation at 37 °C, the MTT solution from each well was removed. A volume of 150 μl DMSO was added, and the plates were shaken for 5 min to dissolve formazan crystals. The optical density at 570 nm for each well was determined using a microtiter plate reader (BioTek, Winooski, VT). Cell viability was represented as the absorbance of treated sample/absorbance of control group × 100 %.

Measurement of cell apoptosis

The percentage of apoptosis for the two cell lines were analyzed by staining with annexin V-FITC and propidium iodide. Both of the cells were seeded in six-well plates at 4×10^5 cells per well. After treatment with the indicated concentrations of curcumin, cells were trypsinized and resuspended in buffer containing 1 % (*v*/*v*) annexin V-FITC and 2 % (*v*/*v*) propidium iodide and incubated in the dark at room temperature for 10 min. Analysis was performed using a flow cytometer (BD Biosciences, Franklin Lakes, NJ, USA), and the characteristics of cells were analyzed by ModFit software (Verity Software House, Topsham, ME, USA).

Assessment of DNA damage

DNA damage was assessed by single cell gel electrophoresis (comet assay) [36]. Briefly, at the end of the curcumin treatment, cells were re-suspended in 0.75 % low melting point (LMP) agarose in phosphate-buffered saline (PBS) (pH 7.4) and placed on microscope slides pre-coated with 0.5 % normal melting point (NMP) agarose. To prevent additional DNA damage, all the steps were conducted under reduced light or in the dark. Cells were lysed for 1 h at 4 °C in a buffer containing 2.5 M NaCl, 100 mM EDTA, 1 % Triton X-100, 10 mM Tris-HCl, and 1 % *N*-lauroylsarcosine sodium, pH 10. Slides were placed in an electrophoresis unit for 40 min to allow DNA to relax in the electrophoretic solution consisting of 300 mM NaOH and 1 mM EDTA, pH>13, at 4 °C. Then, the slides were subjected to electrophoresis (4 °C) for 20 min at electric field strength of 0.86 V/cm, 25 V, 300 mA. After electrophoresis, the slides were neutralized in 0.4 M Tris-HCl (pH 7.5). DNA was stained with PI at a concentration of 2 μg/ml. Slides were analyzed using a fluorescence microscope (Olympus) equipped with a UV-1 filter block at 360 nm connected to the computer-based image analysis system CASP-Comet Assay Software. One hundred images were randomly selected from each sample, and the olive tail moment (OTM) was measured.

Measurement of mitochondrial membrane potential

MMP was measured using the rhodamine 123 fluorescent dye according to the method described previously [37]. Loss of MMP results in the release of rhodamine 123 from the

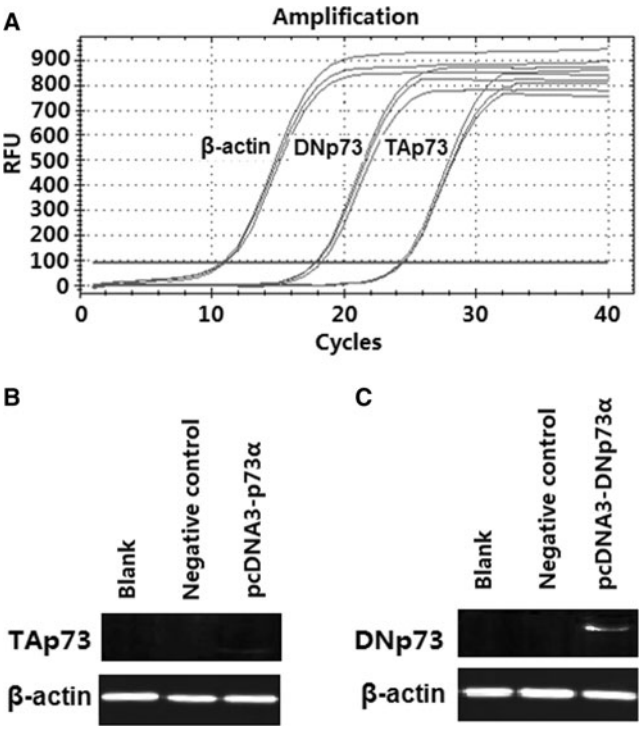

Fig. 1 Hep3B cells were co-transfected with plasmids encoding TAp73 and DNp73. **a** Real-time PCR for detecting the mRNA levels of TAp73 and DNp73 after TAp73 and DNp73 overexpression plasmids co-transfected into Hep3B cells. **b** Western blotting for detecting the protein level of TAp73 after TAp73 and DNp73 overexpression plasmids co-transfected into Hep3B cells; *Blank* without any plasmid, *Negative control* with empty plasmid. **c** Western blotting for detecting the protein level of DNp73 after TAp73 and DNp73 overexpression plasmids co-transfected into Hep3B cells

mitochondria into the cytosol and a resulting increase in intracellular fluorescence [38]. At the end of the curcumin treatment, a total of 1×10^6 cells were harvested and incubated with rhodamine 123 (10 μg/μl) at 37 °C for 30 min in the dark. The rhodamine 123-stained cells were then resuspended in PBS and analyzed directly by flow cytometry.

Western blotting analysis

Expression levels of TAp73, DNp73, cytochrome c, caspase 9, caspase 3, and PARP were analyzed by Western blotting. After treatment with the indicated concentrations of curcumin, 1×10^7 cells were harvested for protein extraction. Mitochondria-free proteins were extracted according to the manufactures' protocols. The whole-cell lysate was extracted with a RIPA buffer (1 M Tris-HCl, 5 M NaCl, 1 % Nonidet P-40, 1 % sodium deoxycholate, 0.05 % SDS, 1 mM phenylmethyl sulfonyl fluoride). The proteins were denatured at 96 °C for 5 min after mixing with 5 μl SDS-loading buffer, separated by 12 % sodium dodecyl sulfate-polyacrylamide gel (SDS-PAGE) and transferred to polyvinylidene fluoride (PVDF) membranes (Millipore, USA). The membranes were

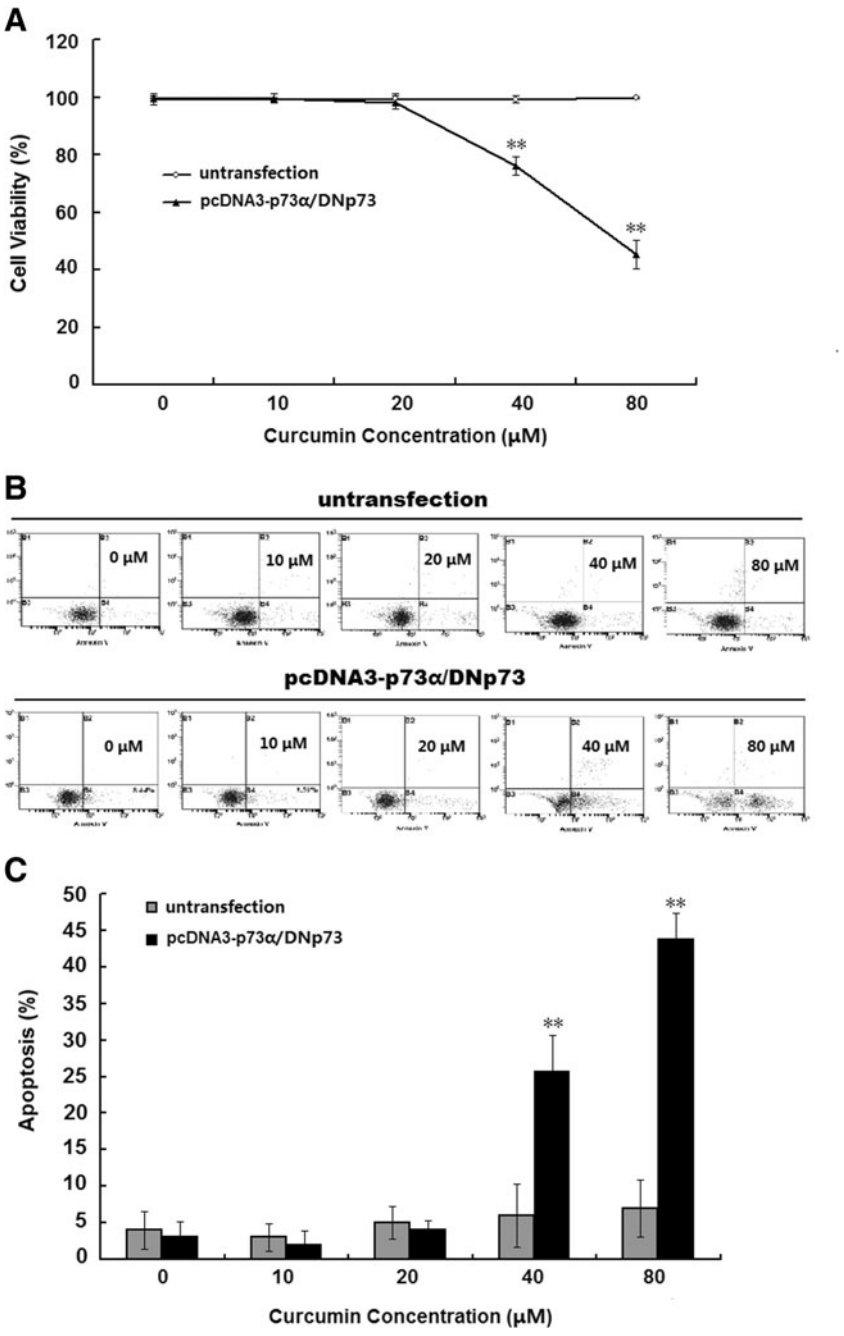

Fig. 2 Both Hep3B and the stable TAp73/DNp73-expressing ($Hep3B^{TAp73/DNp73}$) cells were treated with indicated concentrations of curcumin for 24 h. **a** Cell viability was evaluated by the MTT assay. Mean absorption was normalized to control levels with controls being 100 %. The values represent averages of three independent experiments with six replicate measurements. **b** Representative dot plot of Hep3B and $Hep3B^{TAp73/DNp73}$ cells from three independent experiments. **c** The results of three independent experiments were pooled, and averaged values are shown graphically. Data are presented as mean±SD. $^{**}P<0.01$, compared to control group

then blocked with TBS containing 5 % nonfat milk at 4 °C for 1 h, incubated with the specific primary antibodies (1:400 dilution for all) at 4 °C overnight, then with the corresponding IRDye-conjugated secondary antibodies (1:5000 dilution for all) at room temperature for 1 h. Membranes were visualized using the Odyssey Infrared Imaging System and Odyssey v1.2 (LI-COR, NE, USA). The relative densities of the protein bands were analyzed using Quantity One software (Bio-Rad, CA, USA). The relative expressions of target proteins were normalized to the corresponding intensities of β-actin.

Results

Transfected efficiency of TAp73 and DNp73 expression plasmid

The transfection efficiency in Hep3B after 24-h incubation with TAp73 and DNp73 plasmids was evaluated by Q-PCR and Western blotting methods. The results for Q-PCR are shown in Fig. 1a, for Western blotting are shown in Fig. 1b, c (TAp73 and DNp73, respectively). The mRNA and protein levels in the transfected cells were significantly higher than those in the control cells. Thus, we select the Hep3B$^{TAp73/DNp73}$ cells to study p73 functions in following assays.

Effect of curcumin on cell survival ratio

The cell viability and apoptosis ratio of different concentrations (0, 10, 20, 40, and 80 μM) of curcumin on Hep3B and Hep3B$^{TAp73/DNp73}$ cells were assessed using the MTT reduction assay and annexin V-FITC /PI double-staining assay at 24 h post-treatment. As shown in Fig. 2a, viabilities of Hep3B$^{TAp73/DNp73}$ cells were significantly reduced by 40 and 80 μM curcumin at 24 h ($P<0.01$). However, there was no significant change in the viability at 24 h for all curcumin-treated groups in the Hep3B cells ($P>0.05$). The results of flow cytometry are consistent with the cell viability assay; as shown in Fig. 2b, high levels of apoptotic Hep3B$^{TAp73/DNp73}$ cells were detected in the 40 and 80 μM curcumin-treated groups at 24 h, and these numbers were significantly higher than those observed in the control groups ($P<0.01$) (Fig. 2c); however, compared to the control group, there was no significant change in the apoptotic Hep3B cells at 24 h for all curcumin-treated groups ($P>0.05$). The data were consistent with the cell viability results. Based on the above results, the 24-h time point was chosen for further analyses.

Effect of curcumin on DNA damage

The extent of curcumin-induced DNA damage in Hep3B$^{TAp73/DNp73}$ cells was determined using comet assay. At the top of Fig. 3 are representative immunofluorescent images corresponding to Hep3B$^{TAp73/DNp73}$ cells. At the bottom of Fig. 3 are semi-quantitative representations of the comet images. We found that, compared to the control group, the OTM was significantly increased in 40 and 80 μM curcumin-treated groups ($P<0.05$); however, there was no significant change observed in 10 and 20 μM curcumin-treated groups ($P>0.05$).

Effect of curcumin on MMP

To determine whether curcumin-induced apoptotic cell death was mitochondria associated, the MMP of Hep3B$^{TAp73/DNp73}$ cells was measured using rhodamine 123 staining. As shown in Fig. 4a, increased rhodamine 123-positive Hep3B$^{TAp73/DNp73}$ cells were observed in 40 and 80 μM curcumin-treated groups. The quantitative results are shown in Fig. 4b and indicate that the populations of rhodamine 123-stained cells in the 40 and 80 μM curcumin-treated groups were significantly higher than in the corresponding un-treated groups ($P<0.01$).

Effect of curcumin on protein levels of TAp73 and DNp73

To investigate whether curcumin can activate TAp73 and DNp73, the inductions of TAp73 and DNp73 were examined by Western blotting, and the relative density of the bands was

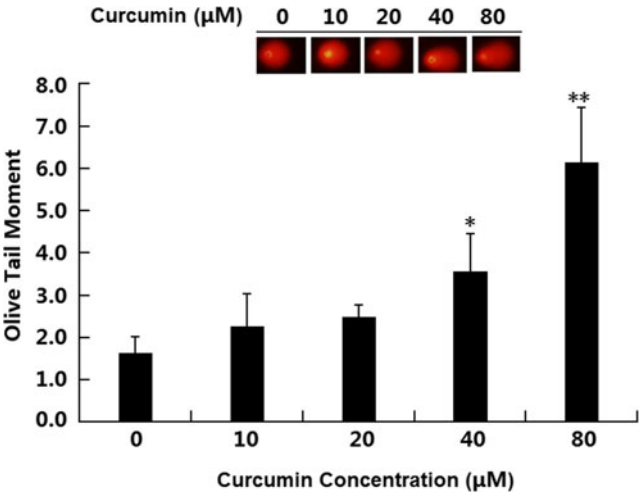

Fig. 3 The Hep3B$^{TAp73/DNp73}$ cell was treated with indicated concentrations of curcumin for 24 h. DNA damage level was assessed by comet assay. Fluorescence images of comets for the Hep3B$^{TAp73/DNp73}$ cells from one of the three independent experiments were presented. The results of three independent experiments were pooled, and averaged values are shown graphically. Data are presented as mean±SD. $^{**}P<0.01$, compared to control group, $^{*}P<0.05$, compared to control group

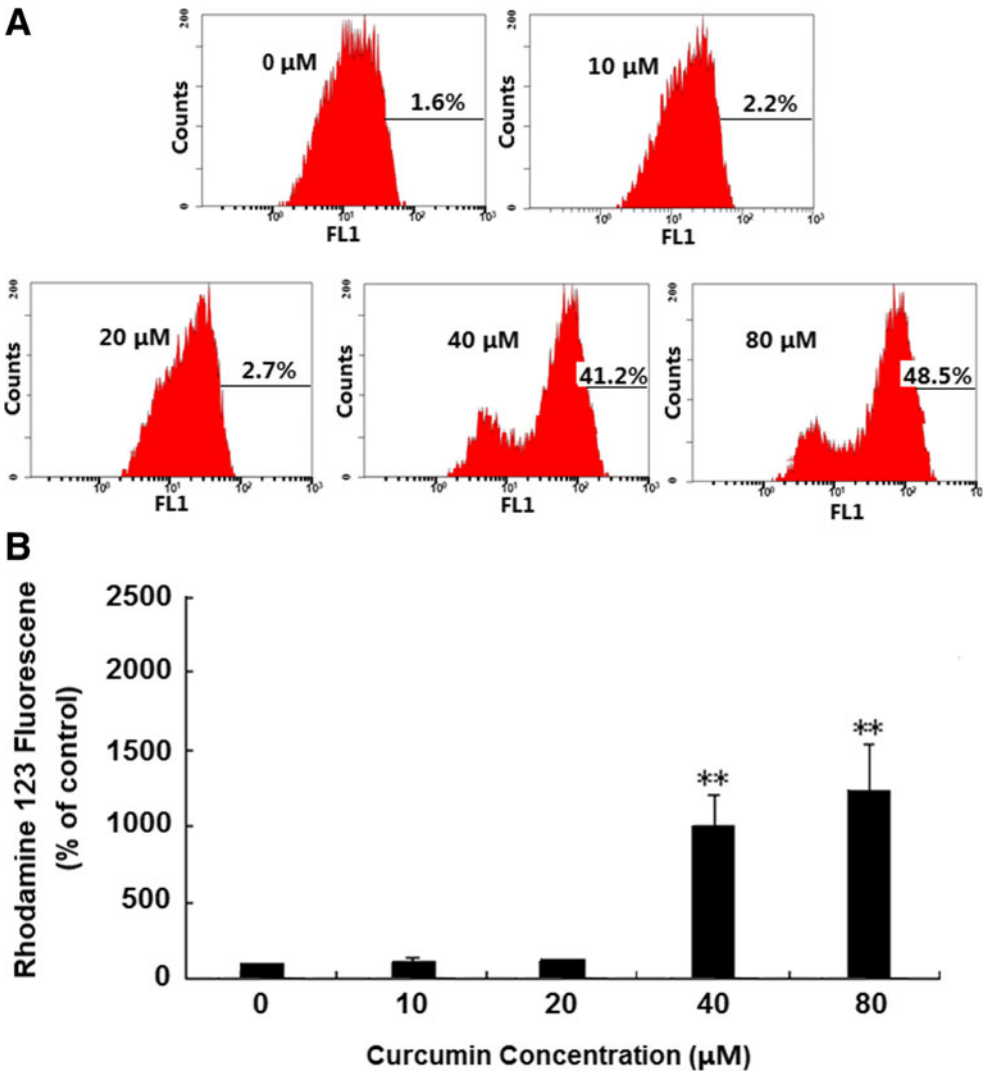

Fig. 4 The Hep3B$^{TAp73/DNp73}$ cell was treated with indicated concentrations of curcumin for 24 h. The mitochondrial membrane potential (MMP) was determined using rhodamine 123 and flow cytometry. **a** Representative dot plot of Hep3B$^{TAp73/DNp73}$ cells from three independent experiments. **b** The results of three independent experiments were pooled, and averaged values are shown graphically. Mean fluorescence was normalized to control levels with controls being 100 %. Data were presented as mean±SD. $^{**}P<0.01$, compared to control group

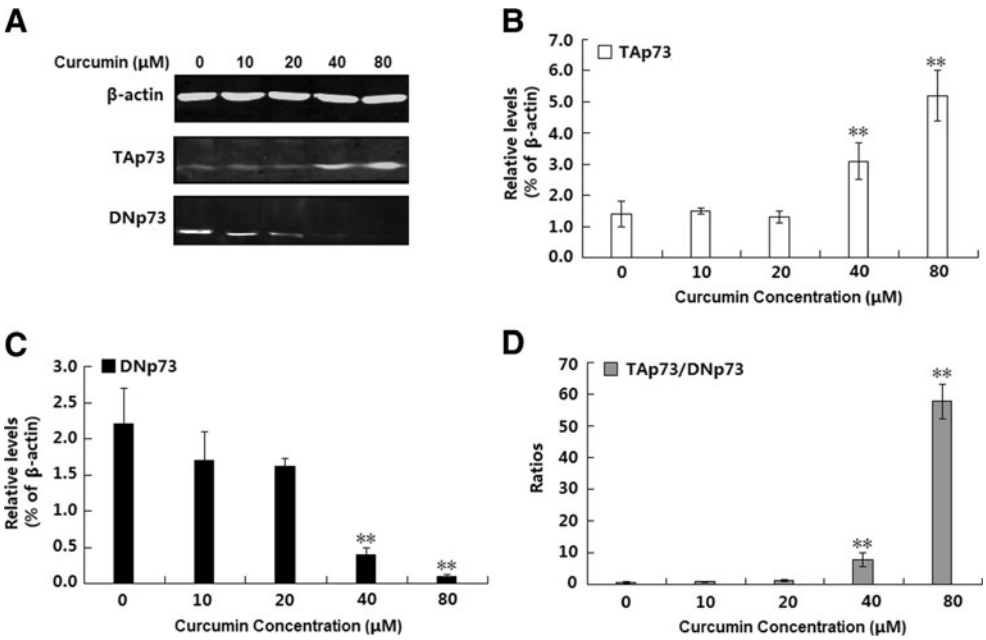

Fig. 5 The Hep3B$^{TAp73/DNp73}$ cell was treated with indicated concentrations of curcumin for 24 h. Western blotting analysis was performed using the corresponding antibodies to check expression and distribution of the proteins. **a** TAp73 and DNp73 protein levels in the whole-cell lysate. **b** Densitometry data for TAp73 expression of three independent experiments were standardized by β-actin. **c** Densitometry data for DNp73 expression of three independent experiments were standardized by β-actin. **d** The ratios of TAp73/DNp73. Data were presented as mean±SD. $^{**}P<0.01$, compared to control group

calculated. After treatment of Hep3B$^{TAp73/DNp73}$ cells with curcumin for 24 h, as shown in Fig. 5a, in the whole-cell lysate, an obvious increase of TAp73 and a corresponding decrease of DNp73 in the 40 and 80 μM curcumin-treated groups were observed; as shown in Fig. 5b, c, compared to the corresponding controls, the differences were significant ($P<0.01$). Additionally, as shown in Fig. 5d, the ratio of TAp73/DNp73 in 40 and 80 μM curcumin-treated groups was also significantly increased ($P<0.01$).

Effect of curcumin on caspases and its associated protein levels

To investigate whether the curcumin-induced apoptosis is caspase associated, the protein levels of caspase 3, cleaved caspase 3, caspase 9, cleaved caspase 9, PARP, and cleaved PARP were examined by Western blotting, and the relative density of the bands was calculated. After treatment of Hep3B$^{TAp73/DNp73}$ cells with curcumin for 24 h, as shown in Fig. 6a, in the whole-cell lysate, curcumin markedly increased cleaved caspase 9, caspase 3, and PARP and obviously decreased pro-caspase 9, pro-caspase 3, and pro-PARP in the 40 and 80 μM curcumin-treated groups ($P<0.01$ for all) (Fig. 6b–d).

Effect of curcumin on cytochrome c release

To investigate whether the curcumin-induced apoptosis is mitochondria dependent, the protein levels of cytochrome c in the mitochondria-free cytosolic extracts were examined by Western blotting, and the relative density of the bands was calculated. After treatment of Hep3B$^{TAp73/DNp73}$ cells with curcumin for 24 h, as shown in Fig. 7a, in the mitochondria-free cytosolic extracts, curcumin markedly increased the cytochrome c released level in the 40 and 80 μM curcumin-treated groups; compared to the control group, the differences were significant ($P<0.01$).

Discussion

Curcumin is a turmeric polyphenol used in cancer therapy and has been reported to induce apoptosis through the activation of p53-dependent pathways [39, 40]. Similar to the previous studies, we found that there is no difference of cell viability after 10–80 μM curcumin 24 h post-treatment in p53-deficient Hep3B cells; however, 40 and

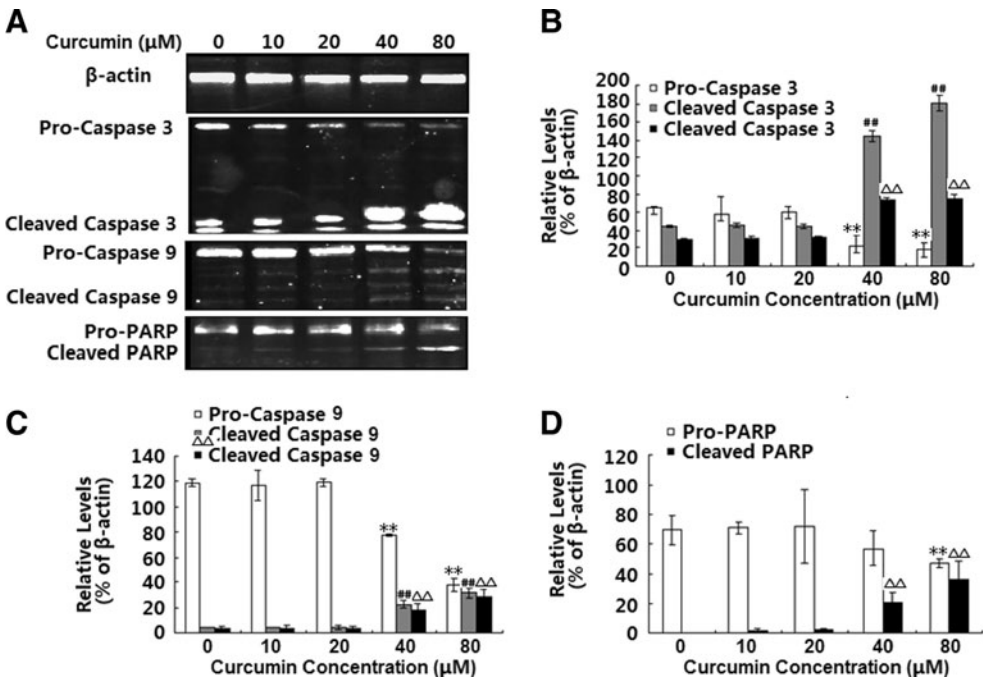

Fig. 6 The Hep3B$^{TAp73/DNp73}$ cell was treated with indicated concentrations of curcumin for 24 h. Western blotting analysis was performed using the corresponding antibodies to check expression of the proteins. **a** Pro-caspase 3, cleaved caspase 3, pro-caspase 9, cleaved caspase 9, pro-PARP, and cleaved PARP protein levels in the whole-cell lysate. **b** Densitometry data for caspase 3 and cleaved caspase 3 protein levels of three independent experiments were standardized by β-actin. **c** Densitometry data for caspase 9 and cleaved caspase 9 protein levels of three independent experiments were standardized by β-actin. **d** Densitometry data for PARP and cleaved PARP protein levels of three independent experiments were standardized by β-actin. Data were presented as mean±SD. $^{**}P<0.01$, compared to control group; $^{\#\#}P<0.01$, compared to control group; $^{\Delta\Delta}P<0.01$, compared to control group

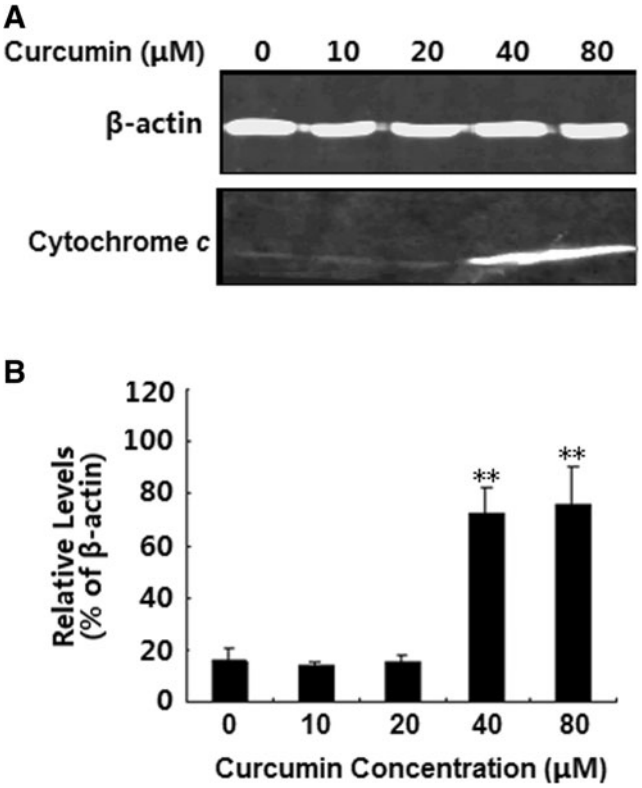

Fig. 7 The Hep3B$^{TAp73/DNp73}$ cell was treated with indicated concentrations of curcumin for 24 h. Western blotting analysis was performed using the corresponding antibodies to check expression of the proteins. **a** Cytochrome c protein levels in mitochondria-free cytosolic extracts. **b** Densitometry data for cytochrome c protein levels of three independent experiments were standardized by β-actin. Data were presented as mean±SD. $^{**}P<0.01$, compared to control group

80 μM curcumin significantly reduced the cell viability in the p53 family member, p73, overexpression Hep3B cells (Hep3B$^{TAp73/DNp73}$). This result was further confirmed by flow cytometry, which demonstrated that c urcumin failed to induce cell death in p53-deficient Hep3B cells, but 40 and 80 μM curcumin induced apoptosis in Hep3B$^{TAp73/DNp73}$ cells after 24 h of treatment.

DNA damage can initiate genomic instability, ultimately leading to cancer [41, 42]. Paradoxically, however, induction of DNA damage is also used to kill cancer cells, and most anticancer agents act by introducing sufficient DNA damage into the cancer cells to activate cell apoptosis [43]. Some anticancer agents can generate DNA damage directly such as cisplatin which can bind to purine bases of DNA leading to mono-, inter-, and intra-strand adducts, causing distortion of the DNA double helix, and ultimately resulting in activation of DNA damage response including cell cycle arrest and apoptosis [44–46]. However, many others generate DNA damage indirectly such as curcumin which can induce ROS generation and results in oxidative DNA damage, ultimately leading to mitotic arrest, apoptosis, and cell cycle arrest [47–52]. The comet assay or single cell gel (SCG) assay is a new method that allows efficient determination of single-strand breaks (SSB) and double-strand breaks (DSB), as well as alkali-labile sites in the DNA of single cells [53, 54]. Thus, comet assay is a sensitive method to determine the extent of DNA damage for recognizing precancerous cells (live cells with unrepaired DNA damage) and to evaluate the effectiveness of anticancer agents (percentage of apoptotic cells). Our data showed that, after 24-h treatment with 40 and 80 μM curcumin, DNA damage extent was increased in which treatment group cell apoptosis was also induced.

p53 plays pivotal roles in connecting the DNA damage response to mitochondria-dependent apoptosis [55, 56]. p73, a p53 family member, has also been predicted to act as a "functional link" due to its significant sequence similarity to p53 [57]. Unlike p53, which is mutated or inactivated in more than 50 % of human tumors, p73 mutations are rarely observed in cancers [28, 57]. Instead, high levels of DNp73 proteins are commonly observed in human tumors, and like p53, TAp73 is a tumor suppressor gene that when specifically deleted in mice (TAp73-/-) leads to enhanced tumor susceptibility [58]. TAp73 also mediates chemotherapy-induced apoptosis, while DNp73 expression leads to chemoresistance [59]. These studies suggest a paradigm in which the balance between the various proapoptotic TAp73 and anti-apoptotic DNp73 isoforms determines whether specific p73 isoform-dependent signaling pathways lead to apoptosis or survival in tumor cells in response to DNA damage. In the present study, we found that curcumin-induced DNA damage caused increase of TAp73 levels but decrease of DNp73 protein levels, resulting in the increase of TAp73/DNp73 ratio. These results, combined with the disruption of MMP; release of cytochrome c from mitochondria; and cleavage of pro-caspase 9, pro-caspase 3, and pro-PARP, indicate that the increased DNA damage contributes to the induction of mitochondria-associated apoptosis via a p73-dependent pathway.

In conclusion, our study demonstrates that curcumin-induced DNA damage accumulation increases TAp73/DNp73 ratio in the TAp73 and DNp73 overexpression Hep3B cells which in turn trigger apoptosis. This curcumin-induced apoptosis is mitochondria associated. Further studies need to be conducted to characterize the detailed mechanisms responsible for p73 activation as well as subsequent events leading to mitochondria-associated apoptosis in response to curcumin.

Acknowledgments This work was supported by grants from National Natural Science Foundation of China (No. 82042282) and grants from Natural Science Foundation of Shandong Province (No. ZR2014HL106).

References

1. Teiten MH, Gaascht F, Eifes S, Dicato M, Diederich M. Chemopreventive potential of curcumin in prostate cancer. Genes Nutr. 2010;5:61–74.
2. Shureiqi I, Baron JA. Curcumin chemoprevention: the long road to clinical translation. Cancer Prev Res (Phila). 2011;4:296–8.
3. Shehzad A, Lee J, Lee YS. Curcumin in various cancers. Biofactors. 2013;39:56–68.
4. Tian F, Song M, Xu PR, Liu HT, Xue LX. [Curcumin promotes apoptosis of esophageal squamous carcinoma cell lines through inhibition of NF-kappaB signaling pathway]. Ai Zheng. 2008;27: 566–70.
5. Swamy MV, Citineni B, Patlolla JM, Mohammed A, Zhang Y, Rao CV. Prevention and treatment of pancreatic cancer by curcumin in combination with omega-3 fatty acids. Nutr Cancer. 2008;60 Suppl 1:81–9.
6. Khar A, Ali AM, Pardhasaradhi BV, Varalakshmi CH, Anjum R, Kumari AL. Induction of stress response renders human tumor cell lines resistant to curcumin-mediated apoptosis: role of reactive oxygen intermediates. Cell Stress Chaperones. 2001;6:368–76.
7. Kang SK, Cha SH, Jeon HG. Curcumin-induced histone hypoacetylation enhances caspase-3-dependent glioma cell death and neurogenesis of neural progenitor cells. Stem Cells Dev. 2006;15:165–74.
8. Lee HE, Han N, Kim MA, Lee HS, Yang HK, Lee BL, et al. DNA damage response-related proteins in gastric cancer: ATM, Chk2 and p53 expression and their prognostic value. Pathobiology. 2014;81: 25–35.
9. Vazquez A, Bond EE, Levine AJ, Bond GL. The genetics of the p53 pathway, apoptosis and cancer therapy. Nat Rev Drug Discov. 2008;7:979–87.
10. Yu X, Robinson JF, Gribble E, Hong SW, Sidhu JS, Faustman EM. Gene expression profiling analysis reveals arsenic-induced cell cycle arrest and apoptosis in p53-proficient and p53-deficient cells through differential gene pathways. Toxicol Appl Pharmacol. 2008;233: 389–403.
11. Li GY, Xie P, Li HY, Hao L, Xiong Q, Qiu T. Involment of p53, Bax, and Bcl-2 pathway in microcystins-induced apoptosis in rat testis. Environ Toxicol. 2011;26:111–7.
12. Lin W, Tongyi S. Role of Bax/Bcl-2 family members in green tea polyphenol induced necroptosis of p53-deficient Hep3B cells. Tumour Biol. 2014;35:8065–75.
13. Vuletic A, Konjevic G, Milanovic D, Ruzdijic S, Jurisic V. Antiproliferative effect of 13-cis-retinoic acid is associated with granulocyte differentiation and decrease in cyclin B1 and Bcl-2 protein levels in G0/G1 arrested HL-60 cells. Pathol Oncol Res. 2010;16:393–401.
14. Jurisic V, Bogdanovic G, Kojic V, Jakimov D, Srdic T. Effect of TNF-alpha on Raji cells at different cellular levels estimated by various methods. Ann Hematol. 2006;85:86–94.
15. He ZY, Shi CB, Wen H, Li FL, Wang BL, Wang J. Upregulation of p53 expression in patients with colorectal cancer by administration of curcumin. Cancer Invest. 2011;29:208–13.
16. Song G, Mao YB, Cai QF, Yao LM, Ouyang GL, Bao SD. Curcumin induces human HT-29 colon adenocarcinoma cell apoptosis by activating p53 and regulating apoptosis-related protein expression. Braz J Med Biol Res. 2005;38:1791–8.
17. Guo LD, Chen XJ, Hu YH, Yu ZJ, Wang D, Liu JZ. Curcumin inhibits proliferation and induces apoptosis of human colorectal cancer cells by activating the mitochondria apoptotic pathway. Phytother Res. 2013;27:422–30.
18. Muller PA, Vousden KH. Mutant p53 in cancer: new functions and therapeutic opportunities. Cancer Cell. 2014;25:304–17.
19. Di Fiore R, Marcatti M, Drago-Ferrante R, D'Anneo A, Giuliano M, Carlisi D, et al. Mutant p53 gain of function can be at the root of dedifferentiation of human osteosarcoma MG63 cells into 3AB-OS cancer stem cells. Bone. 2014;60:198–212.
20. Urist M, Tanaka T, Poyurovsky MV, Prives C. p73 induction after DNA damage is regulated by checkpoint kinases Chk1 and Chk2. Genes Dev. 2004;18:3041–54.
21. Zaika E, Wei J, Yin D, Andl C, Moll U, El-Rifai W, et al. p73 protein regulates DNA damage repair. Faseb J. 2011;25:4406–14.
22. Ferru A, Denis S, Guilhot J, Gibelin H, Tourani JM, Kraimps JL, et al. Expression of TAp73 and DeltaNp73 isoform transcripts in thyroid tumours. Eur J Surg Oncol. 2006;32:228–30.
23. Lo Iacono M, Monica V, Saviozzi S, Ceppi P, Bracco E, Papotti M, et al. p63 and p73 isoform expression in non-small cell lung cancer and corresponding morphological normal lung tissue. J Thorac Oncol. 2011;6:473–81.
24. Bailey SG, Cragg MS, Townsend PA. Family friction as DeltaNp73 antagonises p73 and p53. Int J Biochem Cell Biol. 2011;43:482–6.
25. Zawacka-Pankau J, Kostecka A, Sznarkowska A, Hedstrom E, Kawiak A. p73 tumor suppressor protein: a close relative of p53 not only in structure but also in anti-cancer approach? Cell Cycle. 2010;9:720–8.
26. Grob TJ, Novak U, Maisse C, Barcaroli D, Luthi AU, Pirnia F, et al. Human delta Np73 regulates a dominant negative feedback loop for TAp73 and p53. Cell Death Differ. 2001;8:1213–23.
27. Benosman S, Meng X, Von Grabowiecki Y, Palamiuc L, Hritcu L, Gross I, et al. Complex regulation of p73 isoforms after alteration of amyloid precursor polypeptide (APP) function and DNA damage in neurons. J Biol Chem. 2011;286:43013–25.
28. Rufini A, Agostini M, Grespi F, Tomasini R, Sayan BS, Niklison-Chirou MV, et al. p73 in cancer. Genes Cancer. 2011;2:491–502.
29. Lunghi P, Costanzo A, Mazzera L, Rizzoli V, Levrero M, Bonati A. The p53 family protein p73 provides new insights into cancer chemosensitivity and targeting. Clin Cancer Res. 2009;15:6495–502.
30. Oswald C, Stiewe T. In good times and bad: p73 in cancer. Cell Cycle. 2008;7:1726–31.
31. Boulares AH, Yakovlev AG, Ivanova V, Stoica BA, Wang G, Iyer S, et al. Role of poly(ADP-ribose) polymerase (PARP) cleavage in apoptosis. Caspase 3-resistant PARP mutant increases rates of apoptosis in transfected cells. J Biol Chem. 1999;274:22932–40.
32. Napso T, Fares F. Zebularine induces prolonged apoptosis effects via the caspase-3/PARP pathway in head and neck cancer cells. Int J Oncol. 2014;44:1971–9.
33. Mohan S, Abdul AB, Abdelwahab SI, Al-Zubairi AS, Sukari MA, Abdullah R, et al. Typhonium flagelliforme induces apoptosis in CEMss cells via activation of caspase-9, PARP cleavage and cytochrome c release: its activation coupled with G0/G1 phase cell cycle arrest. J Ethnopharmacol. 2010;131:592–600.
34. Zaika AI, Slade N, Erster SH, Sansome C, Joseph TW, Pearl M, et al. DeltaNp73, a dominant-negative inhibitor of wild-type p53 and TAp73, is up-regulated in human tumors. J Exp Med. 2002;196: 765–80.
35. Sanchez NS, Konigsberg M. Using yeast to easily determine mitochondrial functionality with 1-(4,5-dimethylthiazol-2-yl)-3,5-diphenyltetrazolium bromide (MTT) assay. Biochem Mol Biol Educ. 2006;34:209–12.
36. Dhawan A, Bajpayee M, Parmar D. Comet assay: a reliable tool for the assessment of DNA damage in different models. Cell Biol Toxicol. 2009;25:5–32.
37. Hartig S, Fries S, Balcarcel RR. Reduced mitochondrial membrane potential and metabolism correspond to acute chloroform toxicity of in vitro hepatocytes. J Appl Toxicol. 2005;25:310–7.
38. Nicholls DG. Fluorescence measurement of mitochondrial membrane potential changes in cultured cells. Methods Mol Biol. 2012;810:119–33.

39. Liu E, Wu J, Cao W, Zhang J, Liu W, Jiang X, et al. Curcumin induces G2/M cell cycle arrest in a p53-dependent manner and upregulates ING4 expression in human glioma. J Neurooncol. 2007;85:263–70.
40. Choudhuri T, Pal S, Agwarwal ML, Das T, Sa G. Curcumin induces apoptosis in human breast cancer cells through p53-dependent Bax induction. FEBS Lett. 2002;512:334–40.
41. Roy SS, Chakraborty P, Bhattacharya S. Intervention in cyclophosphamide induced oxidative stress and DNA damage by a flavonyl-thiazolidinedione based organoselenocyanate and evaluation of its efficacy during adjuvant therapy in tumor bearing mice. Eur J Med Chem. 2014;73:195–209.
42. Wang Z, Wang F, Tang T, Guo C. The role of PARP1 in the DNA damage response and its application in tumor therapy. Front Med. 2012;6:156–64.
43. Ronald S, Awate S, Rath A, Carroll J, Galiano F, Dwyer D, et al. Phenothiazine inhibitors of TLKs affect double-strand break repair and DNA damage response recovery and potentiate tumor killing with radiomimetic therapy. Genes Cancer. 2013;4:39–53.
44. Itamochi H, Kigawa J, Akeshima R, Sato S, Kamazawa S, Takahashi M, et al. Mechanisms of cisplatin resistance in clear cell carcinoma of the ovary. Oncology. 2002;62:349–53.
45. Schloffer D, Horky M, Kotala V, Wesierska-Gadek J. Induction of cell cycle arrest and apoptosis in human cervix carcinoma cells during therapy by cisplatin. Cancer Detect Prev. 2003;27:481–93.
46. da Silva GN, de Castro Marcondes JP, de Camargo EA, da Silva Passos Junior GA, Sakamoto-Hojo ET, Salvadori DM. Cell cycle arrest and apoptosis in TP53 subtypes of bladder carcinoma cell lines treated with cisplatin and gemcitabine. Exp Biol Med (Maywood). 2010;235:814–24.
47. Behmand B, Wagner JR, Sanche L, Hunting DJ. Cisplatin intrastrand adducts sensitize DNA to base damage by hydrated electrons. J Phys Chem B. 2014;118:4803–8.
48. Ummat A, Rechkoblit O, Jain R, Roy Choudhury J, Johnson RE, Silverstein TD, et al. Structural basis for cisplatin DNA damage tolerance by human polymerase eta during cancer chemotherapy. Nat Struct Mol Biol. 2012;19:628–32.
49. Thayyullathil F, Chathoth S, Hago A, Patel M, Galadari S. Rapid reactive oxygen species (ROS) generation induced by curcumin leads to caspase-dependent and -independent apoptosis in L929 cells. Free Radic Biol Med. 2008;45:1403–12.
50. Blakemore LM, Boes C, Cordell R, Manson MM. Curcumin-induced mitotic arrest is characterized by spindle abnormalities, defects in chromosomal congression and DNA damage. Carcinogenesis. 2013;34:351–60.
51. Cao J, Liu Y, Jia L, Jiang LP, Geng CY, Yao XF, et al. Curcumin attenuates acrylamide-induced cytotoxicity and genotoxicity in HepG2 cells by ROS scavenging. J Agric Food Chem. 2008;56:12059–63.
52. Lu JJ, Cai YJ, Ding J. Curcumin induces DNA damage and caffeine-insensitive cell cycle arrest in colorectal carcinoma HCT116 cells. Mol Cell Biochem. 2011;354:247–52.
53. Cortes-Gutierrez EI, Hernandez-Garza F, Garcia-Perez JO, Davila-Rodriguez MI, Aguado-Barrera ME, Cerda-Flores RM. Evaluation of DNA single and double strand breaks in women with cervical neoplasia based on alkaline and neutral comet assay techniques. J Biomed Biotechnol. 2012;2012:385245.
54. Benitez-Bribiesca L, Sanchez-Suarez P. Oxidative damage, bleomycin, and gamma radiation induce different types of DNA strand breaks in normal lymphocytes and thymocytes. A comet assay study. Ann N Y Acad Sci. 1999;887:133–49.
55. Zhou M, Gu L, Li F, Zhu Y, Woods WG, Findley HW. DNA damage induces a novel p53-survivin signaling pathway regulating cell cycle and apoptosis in acute lymphoblastic leukemia cells. J Pharmacol Exp Ther. 2002;303:124–31.
56. Chao C, Saito S, Kang J, Anderson CW, Appella E, Xu Y. p53 transcriptional activity is essential for p53-dependent apoptosis following DNA damage. Embo J. 2000;19:4967–75.
57. Moll UM, Slade N. p63 and p73: roles in development and tumor formation. Mol Cancer Res. 2004;2:371–86.
58. Ozaki T, Nakagawara A. p73, a sophisticated p53 family member in the cancer world. Cancer Sci. 2005;96:729–37.
59. Murray-Zmijewski F, Lane DP, Bourdon JC. p53/p63/p73 isoforms: an orchestra of isoforms to harmonise cell differentiation and response to stress. Cell Death Differ. 2006;13:962–72.